Available online at www.sciencedirect.com
SCIENCE DIRECT®
Inorganica Chimica Acta 342 (2003) 37–47
Inorganica Chimica Acta
www.elsevier.com/locate/ica

Mono- and di-functional aromatic amines with *p*-alkoxy substituents as novel arylimido ligands for the hexamolybdate ion

R.A. Roesner [a,*], S.C. McGrath [a], J.T. Brockman [a], J.D. Moll [a], D.X. West [b], J.K. Swearingen [b], A. Castineiras [c]

[a] *Department of Chemistry, Illinois Wesleyan University, Bloomington, IL 61702-2900, USA*
[b] *Department of Chemistry, Illinois State University, Normal, IL 61790-4160, USA*
[c] *Departamento de Quimica Inorganica, Facultad de Quimica, Universidad de Santiago, 15706 Santiago de Compostela, Galicia, Spain*

Received 11 January 2002

Abstract

Mono- and di-functional aromatic amines bearing *p*-alkoxy substituents have been shown to react with the hexamolybdate ion, $[Mo_6O_{19}]^{2-}$, in dry pyridine or acetonitrile (N_2, heat), to form arylimido adducts. The products of these reactions have been characterized by ^1H NMR, IR, and mass spectral studies and, in the case of the *p*-anisidine adduct, X-ray crystallography. The *p*-anisidine adduct, $[Mo_6O_{18}(p\text{-}MeOC_6H_4N)]^{2-}$, has a Mo–N bond length of 1.733(4) Å and an imido (Mo–N–C) bond angle of 163.3(4)°. The *p*-anisidine adduct was crystallized from nitromethane and diethyl ether as the *n*-tetrabutylammonium salt.

Keywords: Polyoxoanions; Crystal structures; Hexamolybdate ion; Imido ligands; Mass spectroscopy; Polyoxometalate

1. Introduction

Polyoxoanions of the early transition metals are widely studied [1] on account of their catalytic activity in a wide variety of reactions; their anti-microbial and anti-tumor properties; their redox activity which makes them useful as corrosion retardants, bleaches, and indicators; and their promise as components in supramolecular systems. The use of polyoxometalates in all of these applications will be enhanced by the ongoing development of reliable methods for attaching organic/bio-organic substituents to the anionic cage. Drugs could be delivered to specific receptor sites, catalysts and indicators could be attached to solid supports or woven into polymers, and molecular scale devices could be assembled from polyoxometalate centers and organic linkages. Organometalic side chains bearing protein-reactive groups have already been used to enhance the specificity of transmission electron microscope stains derived from polyoxometalates [2] and just recently, the incorporation of polyoxometalates into both polymers [3] and dendrimers [4] has been reported.

Organoimido derivatives of the hexamolybdate ion ($Mo_6O_{19}^{2-}$) have been prepared using several different approaches [5]:

$$[Mo_6O_{18}{=}O]^{2-} + R{=}NCO \rightarrow [Mo_6O_{18}{=}NR] + CO_2 \quad (1)$$

$$[Mo_6O_{18}{=}O]^{2-} + RNH_2 \rightarrow [Mo_6O_{18}{=}NR] + H_2O \quad (2)$$

$$[Mo_6O_{18}{=}O]^{2-} + Ph_3P{=}NR \rightarrow [Mo_6O_{18}{=}NR] + Ph_3P{=}O \quad (3)$$

Reactions 1–3 have been used not only to produce a variety of singly substituted species, but also to produce multiply substituted, and bridged species [6]. If hexamolybdate ions are to be incorporated into an increasing variety of supramolecular systems, it will be desirable to develop a variety of μ-imido ligand precursors. Aryl amines and aryl isocyanates are proven starting materials in the preparation of both organoimido ligands with remote functionality [7] and organoimido ligands with extended conjugation [8]. Here we report: (i) reaction of the monofunctional amine, *p*-anisidine, with the hexamolybdate ion to give crystalline $[Mo_6O_{18}(p\text{-}MeOC_6H_4N)]^{2-}$ (Fig. 1); and (ii) our efforts to extend

* Corresponding author. Tel.: +1-309-556 3667
E-mail address: rroesner@titan.iwu.edu (R.A. Roesner).

0020-1693/02/$ - see front matter
PII: S0020-1693(02)01075-7

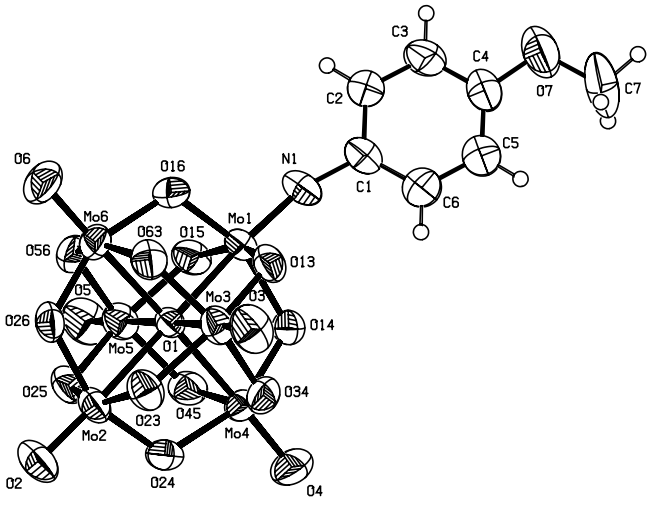

Fig. 1. ORTEP diagram of $[Mo_6O_{18}(p\text{-}MeOC_6H_4N)]^{2-}$.

this chemistry to analogous diamines of varying length (Fig. 2). To our knowledge, this is the first time hexametalate ions have been covalently linked to one another using an extendible family of custom-synthesized, flexible, difunctional ligands. Peng's recent discovery that dicyclohexylcarbodiimide activates reaction of the hexamolybdate ion with amines has been invaluable in this work [9].

2. Experimental

2.1. Materials

Tetrabutylammonium hexamolybdate, $[n\text{-}Bu_4N]_2[Mo_6O_{19}]$, was prepared according to the procedure of Hur et al. [10] or through the procedure of Che et al. [11]. The diamines [1,3-propylene-bis(phenoxy-4-amine); 1,4-butylene-bis(phenoxy-4-amine); and 1,8-octylene-bis(phenoxy-4-amine)] were prepared through combination of the procedures of Bartulín et al. [12] and Griffin et al. [13] as described below. Pyridine was distilled from CaH_2. All other reagents were used as received.

2.2. Instrumentation

NMR spectra were obtained on a 270 MHz JEOL FT-NMR spectrometer. Infrared spectra were collected on a Matteson Genesis Series FT IR. Mass spectra of the organic diamines were obtained using a Hewlett-Packard 6890 Series GC/MS in electron impact mode with an HP-5 crosslinked 5% phenyl methyl siloxane column (30 m long, 0.32 mm i.d.; 0.25 μm thick film). FAB (Fast Atom Bombardment) mass spectra of the polyoxometalates were collected by The University of Kansas Mass Spectrometry Laboratory using a ZAB HS Mass Spectrometer (VG Analytical Ltd., Manchester, UK) equipped with a VAX 4000 data system. FAB experiments were performed using a Xenon gun operated at 8 keV energy and 0.8 mA emission current. The samples were dissolved in MeCN and run in a 3-nitrobenzyl alcohol matrix. C, H, N analyses were performed by Micro-analysis Inc., Wilmington, DE.

2.3. Synthesis of $[n\text{-}Bu_4N]_2[Mo_6O_{18}(p\text{-}MeOC_6H_4N)]$

Dry Py (30 ml) was added to a Schlenk flask and purged for 15 min with a stream of dry nitrogen. Under a blanket of nitrogen, $[n\text{-}Bu_4N]_2[Mo_6O_{19}]$ (0.75 g, 5.5 ×

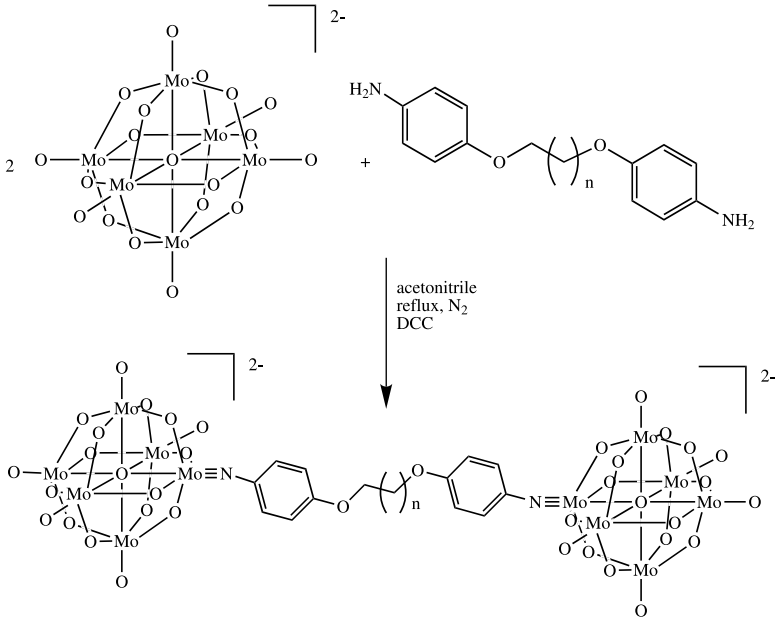

Fig. 2. Diamines of varying length can react with 2 equiv. of the hexamolybdate ion to give bis(hexamolybdate) species.

10^{-4} mol) was added to the stirring Py. After the [n-$Bu_4N]_2[Mo_6O_{19}$] had completely dissolved, 4-methoxyaniline (0.339 g, 2.75×10^{-3} mol) was added to the solution. The resulting reaction mixture was brought to 95 °C and stirred under dry nitrogen for 4 days. The reaction mixture was allowed to cool, and most of the Py was removed under reduced pressure. Diethyl ether (20 ml) was added to the product concentrate giving a dark oil. After vigorous scratching with a glass rod, the oily product solidified into a fine orange powder. The powder was collected by suction filtration and washed with Et_2O (3 × 5 ml), and dried under dynamic vacuum for 2 days to yield 0.77 g (95%). Pure [n-$Bu_4N]_2[Mo_6O_{18}$(*p*-$MeOC_6H_4N$)] was obtained by slow diffusion of Et_2O into a solution of the orange solid (0.090 g) in nitromethane. In addition to dark red crystals of the desired product, [n-$Bu_4N]_2[Mo_6O_{18}$(*p*-$MeOC_6H_4N$)] (0.038 g), yellow crystals of unreacted [n-$Bu_4N]_2[Mo_6O_{19}$] (0.015 g) and orange crystals (0.011 g) were also recovered from the product mixture.

The overall yield of pure [n-$Bu_4N]_2[Mo_6O_{18}$(*p*-$MeOC_6H_4N$)] was 40%: m.p. 221 °C. Negative FAB-MS (3-nitrobenzyl alcohol, MeCN): molecular ion: *m*/*z* 1469 (also 1365, 1227, 1123 and other species). Positive FAB-MS (3-nitrobenzyl alcohol, MeCN): molecular ion: *m*/*z* 1472 (also, 1606, 1711, 1848, 1953 and other species.) ^{1}H NMR (CD_3CN, ppm): δ 0.96 (t, 24H, –CH_3, $[Bu_4N]^+$), 1.36 (m, 16H, –CH_2–, $[Bu_4N]^+$), 1.60 (m, 16H, –CH_2–, $[Bu_4N]^+$), 3.10 (m, 16H, N–CH_2–, $[Bu_4N]^+$), 3.81 (s, ~3H, O–CH_3), 6.90 (d, ~2H, Ar), 7.21 (d, ~2H, Ar). IR (KBr pellet, major absorbances, cm^{-1}): 2963, 2873, 1590, 1486, 1251, 950 (shoulder at 974 is diagnostic for mono-organoimido substituted hexamolybdate [5d,5e]). *Anal*. Calc. for $C_{39}H_{79}Mo_6N_3O_{19}$: C, 31.87; H, 5.42; N, 2.86. Found: C, 31.62; H, 5.42; N, 2.90%.

2.4. Synthesis of 1,4-butylene-bis(phenoxy-4-amine)

1,4-Butylene-bis(phenoxy-4-acetylamide) was synthesized from *p*-hydroxyacetanilide and 1,4-dibromobutane according to the general procedure of Bartulín et al. [12]. The yield based on 30.0 g (0.198 mol) of *p*-hydroxyacetanilide was 23.4 g (66%): ^{1}H NMR (DMSO, ppm): δ 1.84 (br s, 4H, CH_2), 1.97–2.00 (s, 6H, CH_3), 3.98 (s, 4H, O–CH_2), 6.85–6.98 (d, 4H, aromatic), 7.45–7.49 (d, 4H, aromatic), 9.78 (s, 2H, NH). EI MS (MeOH) parent ion: *m*/*z* 356. IR (KBr pellet, major absorbances, cm^{-1}): 3319 (ν_{N-H}), 2958, 2936, 2873 (ν_{C-H}); 1658($\nu_{C=O}$); 1535; 1511; 1239 (ν_{C-O-C} asymmetrical); 1052 (ν_{C-O-C} symmetrical); 973; 832; 715; 606; 542; 521. 1,4-Butylene-bis(phenoxy-4-amine) was prepared from 1,4-butylene-bis(phenoxy-4-acetylamide) through acid hydrolysis of the amide followed by deprotonation of the resultant HCl salt (Griffin et al. [13]). The yield based on 10.0 g (0.281 mol) of 1,4-butylene-bis(phenoxy-4-acetylamide) was 4.27 g (56%): ^{1}H NMR (CD_3CN, ppm): δ 1.82 (pentet, 4H CH_2), 3.78 (br s, 4H, NH_2), 3.89 (t, 4H, O–CH_2), 6.56 (d, 4H, aromatic), 6.69 (d, 4H, aromatic). EI MS (MeOH) molecular ion: *m*/*z* 272. IR (KBr pellet, major absorbances, cm^{-1}): 3394, 3312 (ν_{N-H}); 3215; 2960, 2927, 2863 (ν_{C-N}); 1636; 1512; 1231 (ν_{C-O-C} asymmetrical); 1053 (ν_{C-O-C} symmetrical); 979; 826; 515.

2.5. Synthesis of 1,3-propylene-bis(phenoxy-4-amine)

1,3-Propylene-bis(phenoxy-4-amine) was prepared from *p*-hydroxyacetanilide and 1,3-dibromopropane in 40% yield (not optimized) using the two-step procedure described above for 1,4-butylene-bis(phenoxy-4-amine). ^{1}H NMR (CD_3CN, ppm): δ 2.09 (pentet, 2H, CH_2), 3.79 (br s, 4H, NH_2), 4.01 (t, 4H, O–CH_2), 6.56 (d, 4H, aromatic), 6.70 (d, 4H, aromatic). EI MS (DMSO) molecular ion: *m*/*z* 258. IR (KBr pellet, major absorbances, cm^{-1}): 3399, 3303 (ν_{N-H}); 3201; 2959, 2940, 2887 (ν_{C-N}); 1628; 1515; 1241 (ν_{C-O-C} asymmetrical); 1064 (ν_{C-O-C} symmetrical); 999; 822; 508.

2.6. Synthesis of 1,8-octylene-bis(phenoxy-4-amine)

1,8-Octylene-bis(phenoxy-4-amine) was prepared from *p*-hydroxyacetanilide and 1,8-dibromooctane in 14% yield (not optimized) using the two-step procedure described above for 1,4-butylene-bis(phenoxy-4-amine). ^{1}H NMR (CD_3CN, ppm): δ 1.39 (br, 8H, CH_2), 1.69 (pentet, 4H, CH_2), 3.78 (br s, 4H, NH_2), 3.84 (t, 4H, O–CH_2), 6.56 (d, 4H, aromatic), 6.68 (d, 4H, aromatic). EI MS (DMSO) molecular ion: *m*/*z* 328. IR (KBr pellet, major absorbances, cm^{-1}): 3407, 3311 (ν_{N-H}); 3222; 2932, 2852 (ν_{C-N}); 1636; 1515; 1233 (ν_{C-O-C} asymmetrical); 1064 (ν_{C-O-C} symmetrical); 1016; 935; 516.

2.7. Synthesis of [n-$Bu_4N]_4[Mo_6O_{18}N$–C_6H_4–O–$(CH_2)_4$–O–C_6H_4–NMo_6O_{18}]

This synthesis was performed in a nitrogen atmosphere glove box. To a 100 ml, round bottom flask were added 30 ml of anhydrous MeCN, [n-$Bu_4N]_2[Mo_6O_{19}$] (1.500 g, 1.099×10^{-3} mol), and 1,4-butylene-bis(phenoxy-4-amine) (0.150 g, 5.495×10^{-4} mol). The solution was warmed with a heating mantle and stirred mechanically. After these first two reagents had partially dissolved in the stirring MeCN, 1,3-dicyclohexylcarbodiimide (0.260 g, 1.26×10^{-3} mol) was added. The reaction mixture was brought to reflux and held at reflux for 24 h. The reaction mixture was then cooled to room temperature and allowed to stand for 2 h as a precipitate of 1,3-dicyclohexylurea formed. The reaction mixture was gravity filtered to remove 1,3-dicyclohexylurea and other (dark colored) insoluble materials. The insoluble solids had a mass of 0.284 g. (For comparison,

0.246–0.283 g of 1,3-dicyclohexyl urea is expected, with the exact amount depending on the moisture content of the solvent.) The filtrate was removed from the glove box and rotary evaporated to give a viscous red–brown oil. The oil was dried under dynamic vacuum for 3 days to give a red–brown foam (1.244 g; 76% based on the expected yield of [n-Bu_4N]$_4$[$Mo_6O_{18}N$–C_6H_4–O–$(CH_2)_4$–O–C_6H_4–NMo_6O_{18}]). Positive FAB-MS (3-nitrobenzyl alcohol, MeCN): molecular ion: *m/z* 2958 (molecular weight of [n-Bu_4N]$_4$[$Mo_6O_{18}N$–C_6H_4–O–$(CH_2)_4$–O–C_6H_4–NMo_6O_{18}] = 2965) (also 3207, 2806, 2711, 1850, 1607 and other species). Negative FAB-MS (3-nitrobenzyl alcohol, MeCN): no molecular ion, but 2731, 2489, 1365, 1122, and other species. ^{1}H NMR (CD_3CN, ppm): δ 0.96 (t, 48H, –CH_3, [Bu_4N]$^+$); 1.36 (m, 32H, –CH_2–, [Bu_4N]$^+$); 1.60 (m, 32H, –CH_2–, [Bu_4N]$^+$); $\approx$1.85 (br, small, CH_2, superimposed on base of MeCN resonance); 3.10 (m, 32H, N–CH_2, [Bu_4N]$^+$); 3.91 (t, small, unreacted 1,4-butylene-bis(phenoxy-4-amine)); 4.07 (t, –O–CH_2–); 6.56 (d, small, unreacted 1,4-butylene-bis(phenoxy-4-amine)); 6.68 (d, small, unreacted 1,4-butylene-bis(phenoxy-4-amine)); 6.89 (m, aromatic); 7.19 (d, aromatic). Traces of dicyclohexylurea can be seen in the 1–2 ppm range and at 3.4 ppm. IR (KBr pellet, major absorbances, cm^{-1}): 2968, 2936, 2871, 1629, 1597, 1485, 1244, 954 (shoulder at 974 is diagnostic for mono-organoimido substituted hexamolybdate [5d,5e]), 803. *Anal*. Calc. for [n-Bu_4N]$_4$[$Mo_6O_{18}N$–C_6H_4–O–$(CH_2)_4$–O–C_6H_4–NMo_6O_{18}] (molecular formula = $C_{80}H_{160}Mo_{12}N_6O_{38}$): C, 32.40; H, 5.44; N, 2.83. Found: C, 33.98; H, 5.39; N, 3.32%. *Anal*. Calc. for [n-Bu_4N]$_2$[$Mo_6O_{18}N$–C_6H_4–O–$(CH_2)_4$–O–C_6H_4–NH_2]: C, 35.61; H, 5.60; N, 3.46%.

2.8. Synthesis of [n-Bu_4N]$_4$[$Mo_6O_{18}N$–C_6H_4–O–$(CH_2)_3$–O–C_6H_4–NMo_6O_{18}]

The reaction was conducted according to the procedure described above for [n-Bu_4N]$_4$[$Mo_6O_{18}N$–C_6H_4–O–$(CH_2)_4$–O–C_6H_4–NMo_6O_{18}]. The following quantities of reagents were used: [n-Bu_4N]$_2$[Mo_6O_{19}] (1.500 g, 1.099×10^{-3} mol); 1,3-propylene-bis(phenoxy-4-amine) (0.142 g, 5.495×10^{-4} mol); and 1,3-dicyclohexylcarbodiimide (0.243 g, 1.18×10^{-3} mol). After being held at reflux for 24 h, the reaction mixture was cooled overnight and the insoluble solids (0.265 g) were removed from the reaction mixture by gravity filtration. The filtrate was concentrated under vacuum and then THF was added until a red oil separated from the solution. This oil was removed from the glove box and dried under dynamic vacuum to give a red–brown foam (0.798 g, 49% based on the expected yield of [n-Bu_4N]$_4$[$Mo_6O_{18}N$–C_6H_4–O–$(CH_2)_3$–O–C_6H_4–NMo_6O_{18}]). Positive FAB-MS (3-nitrobenzyl alcohol, MeCN): molecular ion: *m/z* 2944 (molecular weight of [n-Bu_4N]$_4$[$Mo_6O_{18}N$–C_6H_4–O–$(CH_2)_3$–O–C_6H_4–NMo_6O_{18}] = 2951) (also, 3192, 2702, 2177, 2066, 1849, 1608). Negative FAB-MS (3-nitrobenzyl alcohol, MeCN): spectrum was unresolved for *m/z* > 1800. ^{1}H NMR (CD_3CN, ppm): δ 0.94 (t, 48H, –CH_3, [Bu_4N]$^+$); 1.36 (m, 32H, –CH_2–, [Bu_4N]$^+$); 1.60 (m, 32H, –CH_2–, [Bu_4N]$^+$); 3.10 (m, 32H, N–CH_2, [Bu_4N]$^+$); 3.79 (br, unreacted 1,3-propylene-bis(phenoxy-4-amine)); 4.02 (t, unreacted 1,3-propylene-bis(phenoxy-4-amine)); 4.17 (t, –O–CH_2–); 6.56 (d, unreacted 1,3-propylene-bis(phenoxy-4-amine)); 6.68 (d, small, unreacted 1,3-propylene-bis(phenoxy-4-amine)); 6.91 (d, aromatic); 7.18 (d, aromatic). IR (KBr pellet, major absorbances, cm^{-1}): 2964, 2876, 1595, 1483, 1241, 952 (shoulder at 974 is diagnostic for mono-organoimido substituted hexamolybdate [5d,5e]), 806. *Anal*. Calc. for [n-Bu_4N]$_4$[$Mo_6O_{18}N$–C_6H_4–O–$(CH_2)_3$–O–C_6H_4–NMo_6O_{18}] (molecular formula = $C_{79}H_{158}Mo_{12}N_6O_{38}$): C, 32.15; H, 5.40; N, 2.85. Found: C, 31.60; H, 5.31; N, 2.82%. *Anal*. Calc. for [n-Bu_4N]$_2$[$Mo_6O_{18}N$–C_6H_4–O–$(CH_2)_3$–O–C_6H_4–NH_2]: C, 35.18; H, 5.53; N, 3.49%.

2.9. Synthesis of [n-Bu_4N]$_4$[$Mo_6O_{18}N$–C_6H_4–O–$(CH_2)_8$–O–C_6H_4–NMo_6O_{18}]

The reaction was conducted according to the procedure described above for [n-Bu_4N]$_4$[$Mo_6O_{18}N$–C_6H_4–O–$(CH_2)_4$–O–C_6H_4–NMo_6O_{18}]. The following quantities of reagents were used: [n-Bu_4N]$_2$[Mo_6O_{19}] (1.500 g, 1.099×10^{-3} mol); 1,8-octylene-bis(phenoxy-4-amine) (0.180 g, 5.495×10^{-4} mol); and 1,3-dicyclohexylcarbodiimide (0.243 g, 1.18×10^{-3} mol). After being held at reflux for 24 h, the reaction mixture was cooled and allowed to stand for 4 days before the insoluble solids (0.282 g) were removed from the reaction mixture by gravity filtration. The filtrate was concentrated under vacuum (in the glove box) to a volume of approximately 10 ml and THF was added until a red oil separated from the solution. This oil was removed from the glove box and dried under dynamic vacuum to give a red–brown solid (0.821 g, 49% based on the expected yield of [n-Bu_4N]$_4$[$Mo_6O_{18}N$–C_6H_4–O–$(CH_2)_8$–O–C_6H_4–NMo_6O_{18}]). Positive FAB-MS (3-nitrobenzyl alcohol, MeCN): the molecular ion did not give a well-resolved signal, but a signal at *m/z* = 3263 corresponds to ([n-Bu_4N]$_5$[$Mo_6O_{18}N$–C_6H_4–O–$(CH_2)_8$–O–C_6H_4–NMo_6O_{18}])$^+$. Other prominent signals include 2720, 1848, and 1608. Negative FAB-MS (3-nitrobenzyl alcohol, MeCN): spectrum was unresolved for *m/z* > 1800. ^{1}H NMR (CD_3CN, ppm): δ 0.94 (t, 48H, –CH_3, [Bu_4N]$^+$); 1.37 (m, 32H, –CH_2–, [Bu_4N]$^+$); 1.61 (m, 32H, –CH_2–, [Bu_4N]$^+$); 3.10 (m, 32H, N–CH_2, [Bu_4N]$^+$); 3.84 (triplet, unreacted 1,8-octylene-bis(phenoxy-4-amine)); 4.01 (t, –O–CH_2–); 6.56 (d, unreacted 1,8-octylene-bis(phenoxy-4-amine)); 6.68 (d, small, unreacted 1,8-octylene-bis(phenoxy-4-amine)); 6.88 (d,

aromatic); 7.19 (d, aromatic). IR (KBr pellet, major absorbances, cm^{-1}): 2965, 2867, 1595, 1475, 1249, 954 (shoulder at 975 is diagnostic for mono-organoimido substituted hexamolybdate [5d,5e]), 790. *Anal*. Calc. for a sample of [n-Bu_4N]$_4$[$Mo_6O_{18}N$–C_6H_4–O–$(CH_2)_8$–O–C_6H_4–NMo_6O_{18}] (molecular formula = $C_{84}H_{168}Mo_{12}N_6O_{38}$): C, 33.39; H, 5.60; N, 2.78. Found: C, 33.31; H, 5.58; N, 2.83%. *Anal*. Calc. for [n-Bu_4N]$_2$[$Mo_6O_{18}N$–C_6H_4–O–$(CH_2)_8$–O–C_6H_4–NH_2]: C, 37.29; H, 5.90; N, 3.34%.

2.10. X-ray data collection and reduction for [n-Bu_4N]$_2$[Mo_6O_{18}(*p*-$MeOC_6H_4N$)]

A red–brown prismatic crystal of [n-Bu_4N]$_2$-[Mo_6O_{18}(*p*-$MeOC_6H_4N$)] (obtained from gaseous diffusion of Et_2O into a nitromethane solution of the compound) was mounted on a glass fiber and used for data collection. Cell constants and an orientation matrix for data collection were obtained by least-squares refinement of the diffraction data from 25 reflections in the range of $2.63 < \theta < 14.41^\circ$ in a Enraf–Nonius MACH3 automatic diffractometer [14]. Data were collected at 293 K using Mo Kα radiation ($\lambda = 0.71073$ Å) and the ω-scan technique, and corrected for Lp effects [15]. A semi-empirical absorption correction (Ψ-scans) was made [16].

2.11. Structure solution and refinement for [n-Bu_4N]$_2$[Mo_6O_{18}(*p*-$MeOC_6H_4N$)]

The structure was solved by direct methods [17] and subsequent difference Fourier maps, and refined on F^2 by a full-matrix least-squares procedure using anisotropic displacement parameters [18]. One of the carbon atom chains, C81–C82–C83–C84, of a tetrabutylammonium cation showed disorder and was refined with fixed position parameters for the four carbon atoms. All hydrogen atoms were located in their calculated positions (C–H 0.93–0.97 Å) and were refined using a riding model. Atomic scattering factors were taken from the 'International Tables for X-ray Crystallography' [19]. Molecular graphics were generated using PLATON-98 [20]. A summary of the crystal data, experimental details, and refinement results are listed in Table 1.

Table 1
Crystal data, data collection, and refinement parameters for [n-Bu_4N]$_2$[Mo_6O_{18}(*p*-$MeOC_6H_4N$)]

Empirical formula	$C_{39}H_{79}Mo_6N_3O_{19}$
Formula weight	1469.69
Temperature (K)	293(2)
Wavelength (Å)	0.71073
Crystal system	monoclinic
Space group	$P2_1/c$ (no. 14)
a (Å)	17.599(3)
b (Å)	15.577(9)
c (Å)	20.682(7)
α (°)	90
β (°)	104.91(3)
γ (°)	90
V (Å^3)	5479(4)
Z	4
D_{calc} (g cm^{-3})	1.782
Absorption coefficient (mm^{-1})	1.400
$F(000)$	2952
Crystal size (mm)	0.20 × 0.20 × 0.20
θ Range for data collection (°)	1.36–27.54
Index ranges	$0 \le h \le 22$, $0 \le k \le 20$, $-26 \le l \le 25$
Reflections collected	13 041
Reflections unique	12 578 [$R_{int} = 0.0221$]
Completeness to $2\theta = 27.54$	95.9%
Max./min. transmission	0.775 and 0.360
Refinement method	full-matrix least-squares on F^2
Data/restraints/parameters	12 578/0/601
Final R indices [$I > 2\sigma(I)$]	$R_1 = 0.0386$, $wR_2 = 0.0933$
R indices (all data)	$R_1 = 0.0820$, $wR_2 = 0.1090$
Goodness-of-fit on F^2	1.010
Largest difference peak and hole (e Å^{-3})	0.744 and −0.514

3. Results and discussion

3.1. Synthesis and characterization of [n-Bu_4N]$_2$[Mo_6O_{18}(*p*-$MeOC_6H_4N$)]

[n-Bu_4N]$_2$[Mo_6O_{18}(*p*-$MeOC_6H_4N$)] (Fig. 1) was synthesized to demonstrate that *p*-alkoxy substituted anilines can serve as organoimido ligand precursors for the hexamolybdate ion. The synthesis and characterization of [n-Bu_4N]$_2$[Mo_6O_{18}(*p*-$MeOC_6H_4N$)] also provides a basis for understanding the more complex materials that form when the hexamolybdate ion is reacted with structurally analogous, difunctional amines (vide infra). Although the analytical, spectroscopic, and structural data reported here is for a sample of [n-Bu_4N]$_2$[Mo_6O_{18}(*p*-$MeOC_6H_4N$)] that was prepared in dry pyridine and recrystallized from nitromethane/diethyl ether (Section 2.3), we later demonstrated that nearly pure [n-Bu_4N]$_2$[Mo_6O_{18}(*p*-$MeOC_6H_4N$)] could be obtained directly when [n-Bu_4N]$_2$[Mo_6O_{19}] was reacted with 4-methoxyaniline in the presence of dicyclohexylcarbodiimide according to the procedure of Peng and co-workers [5c].

The ^{1}H NMR spectrum of [n-Bu_4N]$_2$[Mo_6O_{18}(*p*-$MeOC_6H_4N$)] is characterized by significant downfield shifts of the aromatic and methoxy hydrogens relative to free 4-methoxyaniline. In CD_3CN, the aromatic doublets shift from 6.6 and 6.7 ppm to 6.9 and 7.2 ppm while the methoxy resonance shifts from 3.7 to 3.8 ppm.

Similar downfield shifts are seen by Errington and co-workers in the reaction 1,4-phenylene diamine with the hexamolybdate ion [6b]. By comparing integral values of ligand resonances to integral values of the n-tetrabutylammonium ion resonances, the extent of organoimido substitution can be easily quantified. In this way, we were able to determine that the crude orange powder had a hexamolybdate ion to ligand ratio of approximately 2:1, while the purified, red, crystalline product had a hexamolybdate ion to ligand ratio of 1:1.

The IR spectrum of $[n\text{-}Bu_4N]_2[Mo_6O_{18}(p\text{-}MeOC_6H_4N)]$ shows both the strong Mo–O stretch of the hexamolybdate ion at 950 cm^{-1} and a shoulder at 974 cm^{-1} that is diagnostic for mono-organoimido substitution [5d,5e].

We have found that hexamolybdate-containing species can be detected easily using FAB-MS. Because molybdenum has seven stable isotopes (with natural abundances ranging from 9.25 to 24.13%) [21], each chemical species containing one hexamolybdate ion gives a statistically distributed cluster of signals that is approximately 40 mass units wide. While ideally these clusters have a Gaussian shape with the apex corresponding to the calculated monoisotopic mass of the compound, in practice these clusters often have slightly less-regular shapes. The negative FAB mass spectrum of $[n\text{-}Bu_4N]_2[Mo_6O_{18}(p\text{-}MeOC_6H_4N)]$ (3-nitrobenzyl alcohol, acetonitrile) shows signals for: the molecular ion ($m/z = 1469$); $([n\text{-}Bu_4N][Mo_6O_{18}(p\text{-}MeOC_6H_4N)])^-$ ($m/z = 1227$); unsubstituted $([n\text{-}Bu_4N]_2[Mo_6O_{19}])^-$ ($m/z = 1365$); and unsubstituted $([n\text{-}Bu_4N][Mo_6O_{19}])^-$ ($m/z = 1123$). When detection of positive ions is employed, the FAB mass spectrum shows signals for: the molecular ion ($m/z = 1472$); $([n\text{-}Bu_4N]_3[Mo_6O_{18}(p\text{-}MeOC_6H_4N)])^+$ ($m/z = 1711$); $([n\text{-}Bu_4N]_4[Mo_6O_{18}(p\text{-}MeOC_6H_4N)])^+$ ($m/z = 1953$); unsubstituted $([n\text{-}Bu_4N]_3[Mo_6O_{19}])^+$ ($m/z = 1606$); and unsubstituted $([n\text{-}Bu_4N]_4[Mo_6O_{19}]-H)^+$ ($m/z = 1848$). Our observations that the negative detection technique shows prominent signals for species 'missing' tetrabutylammonium ions, while the positive detection technique shows prominent signals for species with 'extra' tetrabutylammonium ions hold true for all of the substituted tetrabutylammonium hexamolybdates studied.

As mentioned in Section 2.3, recrystallization of crude $[n\text{-}Bu_4N]_2[Mo_6O_{18}(p\text{-}MeOC_6H_4N)]$ afforded three types of crystals which were subsequently sorted from one another mechanically using a pin and a dissecting microscope. In addition to the red–brown crystals of $[n\text{-}Bu_4N]_2[Mo_6O_{18}(p\text{-}MeOC_6H_4N)]$ for which we report an X-ray crystal structure (vide infra), we also obtained yellow crystals of unsubstituted $[n\text{-}Bu_4N]_2[Mo_6O_{19}]$ and orange crystals which were found by MS and ^1H NMR to be a mixture of $[n\text{-}Bu_4N]_2[Mo_6O_{19}]$ and $[n\text{-}Bu_4N]_2[Mo_6O_{18}(p\text{-}MeOC_6H_4N)]$. By ^1H NMR integration, the orange crystals are 69% $[n\text{-}Bu_4N]_2[Mo_6O_{19}]$ and 31% $[n\text{-}Bu_4N]_2[Mo_6O_{18}(p\text{-}MeOC_6H_4N)]$. A similar co-crystallization phenomenon has been reported by Proust et al. for $[n\text{-}Bu_4N]_2[Mo_6O_{18}(NPh)]$, $[n\text{-}Bu_4N]_2[cis\text{-}Mo_6O_{17}(NPh)_2]$, and $[n\text{-}Bu_4N]_2[Mo_6O_{19}]$ [5d].

An ORTEP diagram of the $[Mo_6O_{18}(p\text{-}MeOC_6H_4N)]^{2-}$ anion is shown in Fig. 1 and selected bond lengths and angles are presented in Table 2. The C(1)–N(1)–Mo(1) angle of 163.3(4)° is consistent with angles observed for other para-only substituted arylimido ligands [3b,7a,5e] and substantially smaller than the angles observed for various bis(ortho-substituted) arylimido ligands [5a,8a,9] (Table 3). The more linear C–N–Mo bond angles observed for the latter ligands are not necessarily accompanied by shorter Mo–N bond lengths, as might be expected considering the sp hybridization of the imido nitrogen atom and a formal Mo–N triple bond. This suggests that the C–N–Mo bond angle may be more closely related to steric constraints imposed by the ortho substituents than to absolute Mo–N bond strength.

Other structural feature of substituted Lindqvist (hexametalate) ions which are noteworthy include: (i) geometric distortions in the ion's symmetry caused by substitution; and (ii) alternation of molybdenum–O_b (bridging oxygen) bond lengths around the equatorial belt of the ion (the belt that does not include the imido ligand). The central oxygen atom, O_C, of mono-substituted Lindqvist ions is typically displaced towards the site of substitution [3b,5a,5c,5d,5e,6a,6c,8a,22–29] and $[n\text{-}Bu_4N]_2[Mo_6O_{18}(p\text{-}MeOC_6H_4N)]$ is typical in this regard with its Mo(1)–O(1) bond length of 2.213(3) Å being significantly shorter than the other Mo–O_C bonds lengths of 2.355(3), 2.342(3), 2.313(3), 2.318(3), and 2.330(3) Å. This distortion has been attributed to the greater trans-influence of the terminal oxo ligand relative to the imido ligand [5d]. Displacement of the central oxygen atom is often accompanied by variations in the molybdenum–O_b bond distances going around the longitudinal belts of the ion (the belts that contain the Mo≡NR unit), with the Mo(NR)–O_b bond distances being longer than the other molybdenum–O_b bond distances [5a,29]. The schematic diagram in Fig. 3 shows these geometric distortions for $[n\text{-}Bu_4N]_2[Mo_6O_{18}(p\text{-}MeOC_6H_4N)]$. The reported Mo(1)–$O_b$ bond length of 1.944 Å is the mean for Mo(1)–O(13), Mo(1)–O(14), Mo(1)–O(15), and Mo(1)–O(16). The other mean bond lengths were calculated in a similar manner. Like many other Lindqvist anions, $[n\text{-}Bu_4N]_2[Mo_6O_{18}(p\text{-}MeOC_6H_4N)]$ shows an alternating long–short pattern in molybdenum–O_b bond lengths around the equatorial belt [30,31]. These are illustrated in Fig. 4.

Table 2
Selected bond distances (Å) and angles (°) for $[n\text{-}Bu_4N]_2[Mo_6O_{18}(p\text{-}MeOC_6H_4N)]$

Bond lengths	
Mo(1)–N(1)	1.733(4)
Mo(1)–O(16)	1.898(3)
Mo(1)–O(15)	1.919(3)
Mo(1)–O(14)	1.973(3)
Mo(1)–O(13)	1.988(3)
Mo(1)–O(1)	2.213(3)
Mo(2)–O(2)	1.671(3)
Mo(2)–O(23)	1.880(3)
Mo(2)–O(24)	1.882(3)
Mo(2)–O(26)	1.950(3)
Mo(2)–O(25)	1.950(3)
Mo(2)–O(1)	2.355(3)
Mo(3)–O(3)	1.686(4)
Mo(3)–O(13)	1.862(3)
Mo(3)–O(63)	1.919(3)
Mo(3)–O(34)	1.947(3)
Mo(3)–O(23)	1.953(3)
Mo(3)–O(1)	2.342(3)
Mo(4)–O(4)	1.685(3)
Mo(4)–O(14)	1.872(3)
Mo(4)–O(34)	1.921(4)
Mo(4)–O(45)	1.936(4)
Mo(4)–O(24)	1.948(3)
Mo(4)–O(1)	2.313(3)
Mo(5)–O(5)	1.675(4)
Mo(5)–O(25)	1.902(3)
Mo(5)–O(45)	1.921(3)
Mo(5)–O(56)	1.926(3)
Mo(5)–O(15)	1.931(3)
Mo(5)–O(1)	2.318(3)
Mo(6)–O(6)	1.684(3)
Mo(6)–O(26)	1.892(3)
Mo(6)–O(56)	1.922(3)
Mo(6)–O(63)	1.936(3)
Mo(6)–O(16)	1.938(3)
Mo(6)–O(1)	2.330(3)
Bond angles	
C(1)–N(1)–Mo(1)	163.3(4)
Mo(1)–O(1)–Mo(4)	91.36(10)
Mo(1)–O(1)–Mo(5)	90.68(10)
Mo(4)–O(1)–Mo(5)	90.24(10)
Mo(1)–O(1)–Mo(6)	90.87(9)
Mo(4)–O(1)–Mo(6)	177.74(13)
Mo(5)–O(1)–Mo(6)	90.10(9)
Mo(1)–O(1)–Mo(3)	90.82(9)
Mo(4)–O(1)–Mo(3)	90.12(9)
Mo(5)–O(1)–Mo(3)	178.44(13)
Mo(6)–O(1)–Mo(3)	89.48(9)
Mo(1)–O(1)–Mo(2)	179.91(18)
Mo(4)–O(1)–Mo(2)	88.70(9)
Mo(5)–O(1)–Mo(2)	89.39(9)
Mo(6)–O(1)–Mo(2)	89.06(9)
Mo(3)–O(1)–Mo(2)	89.11(10)
Mo(3)–O(13)–Mo(1)	114.85(15)
Mo(4)–O(14)–Mo(1)	114.72(14)
Mo(1)–O(15)–Mo(5)	113.71(16)
Mo(1)–O(16)–Mo(6)	115.14(15)
Mo(2)–O(23)–Mo(3)	118.54(16)
Mo(2)–O(24)–Mo(4)	116.89(15)
Mo(5)–O(25)–Mo(2)	117.15(15)
Mo(6)–O(26)–Mo(2)	117.58(15)
Mo(4)–O(34)–Mo(3)	116.82(15)

Table 2 *(Continued)*

Bond angles	
Mo(5)–O(45)–Mo(4)	116.66(16)
Mo(6)–O(56)–Mo(5)	117.54(16)
Mo(3)–O(63)–Mo(6)	117.14(16)
Mo(1)–O(13)–Mo(3)	114.85(15)
Mo(1)–O(14)–Mo(4)	114.72(14)
Mo(1)–O(15)–Mo(5)	113.71(16)
Mo(1)–O(16)–Mo(6)	115.14(15)

Table 3
Mo–N–C bond angles and Mo–N bond lengths for several organoimido polyoxomolybdates

Polyoxoanion (2-)	Mo-N-C bond angle (°)	Mo-N bond length (Å)	Reference
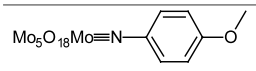	163.3(4)	1.733(4)	This work
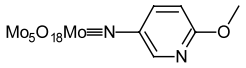	163.7(7)	1.724(6)	7a
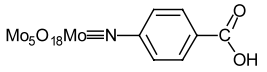	158.0(12)	1.752(13)	7a
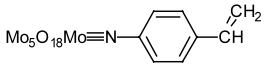	159.9(7)	1.728(7)	3b
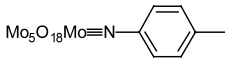	154.2(16)	1.661(18)	5e
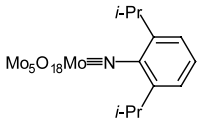	176.3(15)	1.739(15)	5a
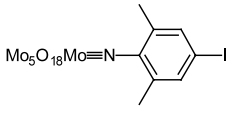	172.8(6)	1.733(6)	9
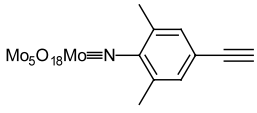	172.5(5)	1.729(5)	9
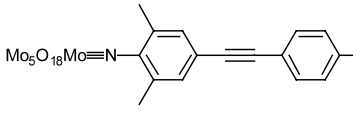	171.4(18)	1.739(19)	8a

3.2. Synthesis and characterization of the bis(hexamolybdate) complexes (a.k.a. dumbbells): $[n\text{-}Bu_4N]_4[Mo_6O_{18}N–C_6H_4–O–(CH_2)_n–O–C_6H_4–NMo_6O_{18}]$

The bis(hexamolybdate) complexes, $[n\text{-}Bu_4N]_4[Mo_6O_{18}N–C_6H_4–O–(CH_2)_n–O–C_6H_4–NMo_6O_{18}]$, are but one group of compounds which may theoretically form when the hexamolybdate ion, with its six reactive terminal oxo ligands, is allowed to react with

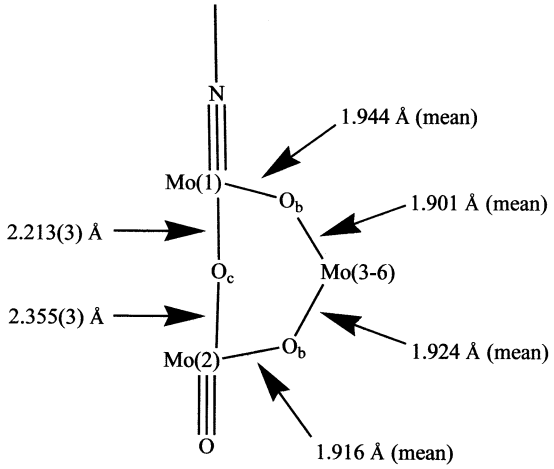

Fig. 3. Geometric distortions in $[n\text{-}Bu_4N]_2[Mo_6O_{18}(p\text{-}MeOC_6H_4N)]$. The reported Mo(1)–$O_b$ bond length of 1.944 Å is the mean for Mo(1)–O(13), Mo(1)–O(14), Mo(1)–O(15), and Mo(1)–O(16). The other mean bond lengths were calculated in a similar manner.

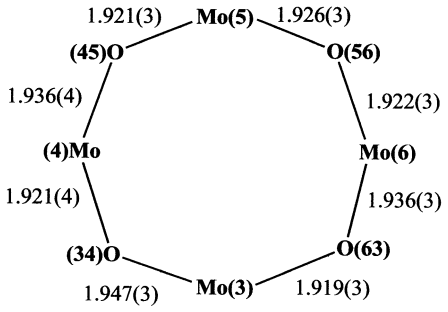

Fig. 4. Alternating long–short bonding pattern around the equatorial belt of $[n\text{-}Bu_4N]_2[Mo_6O_{18}(p\text{-}MeOC_6H_4N)]$.

flexible difunctional amines. Polyfunctionalized hexamolybdate ions, polymers, oligomers, and 'basket-handle species' (compounds in which a single diamine has reacted with two *cis*-sites on the same hexamolybdate) are some of the other possibilities. If all of these species were, in fact, equally likely to form, the preparation of any one of these compounds would be a truly formidable task. In actuality, each successive organoimido substitution of the hexamolybdate ion requires substantially more forcing conditions, such that stoichiometry, temperature, and reaction time can be used to gain some control over these substitution processes [5a,5b,6c]. While we have been unable to isolate analytically pure samples of the bis(hexamolybdate) species, analysis of the crude materials provides valuable information.

FAB mass spectra suggest that the proposed bis(hexamolybdate) species, $[n\text{-}Bu_4N]_4[Mo_6O_{18}N\text{–}C_6H_4\text{–}O\text{–}(CH_2)_n\text{–}O\text{–}C_6H_4\text{–}NMo_6O_{18}]$, are significant components of the crude products. Just as the positive FAB mass spectrum of $[n\text{-}Bu_4N]_2[Mo_6O_{18}(p\text{-}MeOC_6H_4N)]$ contains a medium sized signal for the molecular ion (1472) and a very prominent signal for $[n\text{-}Bu_4N]_3[Mo_6O_{18}(p\text{-}MeOC_6H_4N)]^+$ (1711); the +FAB mass spectra of the dumbbells each have especially prominent signals for $[n\text{-}Bu_4N]_5[Mo_6O_{18}N\text{–}C_6H_4\text{–}O\text{–}(CH_2)_n\text{–}O\text{–}C_6H_4\text{–}NMo_6O_{18}]^+$ (Table 4). While we were generally unable to detect high molecular weight species ($m/z > 1700$) in the −FAB mass spectra, the signals observed for the product of $[n\text{-}Bu_4N]_2[Mo_6O_{19}]$ reacting with 1,4-butylene-bis(phenoxy-4-amine) support formation of a bis(hexamolybdate) product. The mass spectra of the products were also examined for evidence of simple hexamolybdate–diamine adducts, $[n\text{-}Bu_4N]_2[Mo_6O_{18}N\text{–}C_6H_4\text{–}O\text{–}(CH_2)_n\text{–}O\text{–}C_6H_4\text{–}NH_2]$, and basket handle species (Fig. 5) [32]. With the possible exception of the 1,8-octylene-bis(phenoxy-4-amine) based 'basket handle' species, there is no mass spectral evidence to suggest formation of these 1:1 hexamolybdate–diamine adducts. Oligomers containing three or more hexamolybdate ions were beyond our detection range for this series of mass spectral experiments. The widths of the isotopic distribution patterns in our mass spectra also support the formation of bis(hexamolybdate) species. Whereas the signal for $[n\text{-}Bu_4N]_2[Mo_6O_{19}]$ is expected to be 42 mass units wide, the signals for the bis(hexamolybdate) species are expected to be approximately 60 mass units wide. These differences in width can be seen clearly in our spectra.

Table 4
Selected mass spectral data for the organoimido hexamolybdates

	Molecular ion (calculated)	Molecular ion + $[Bu_4N]^+$ (calculated)	Molecular ion − $[Bu_4N]^+$ (calculated)	Selected +FAB signals	Selected −FAB signals
$[n\text{-}Bu_4N]_2[Mo_6O_{18}(p\text{-}MeOC_6H_4N)]$	1470	1712	1227	1472 1711	1473 1228
'C_3' dumbbell	2952	3194	2709	2944 3192	
'C_4' dumbbell	2966	3208	2723	2958 3207	2731 2489 [a]
'C_8' dumbbell	3022	3264	2779	3263	

[a] (2731 − $[Bu_4N]^+$).

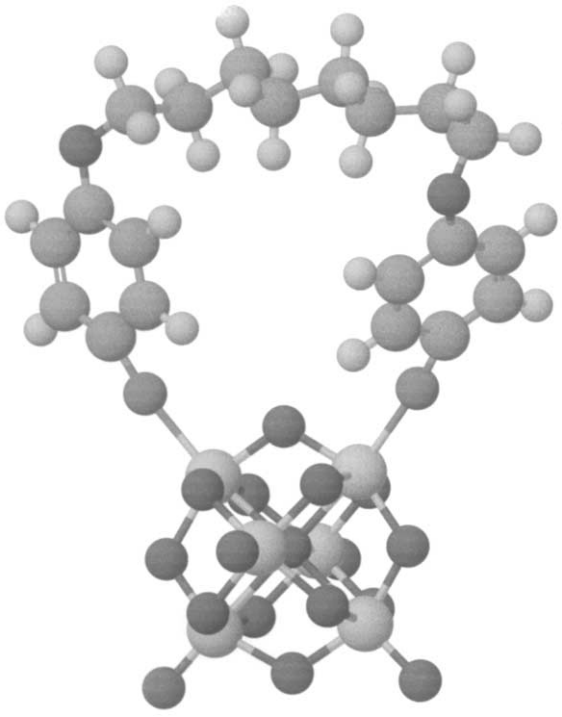

Fig. 5. Optimized structure of the C8 basket-handle species generated using MM2 parameters in Personal CAChe. The atomic positions of the Mo–O framework were taken from Maatta's X-ray data for $[Mo_6O_{17}(NAr)_2]^{2-}$ [5a] and those positions were locked for subsequent minimizations. The Mo≡N–C bond angles were fixed at 170° while the remainder of the organic ligand was geometrically unconstrained. The eight-membered methylene strap had C–C single bond lengths of 1.54 Å and C–C–C bond angles ranging from 111.68 to 114.64°.

The ^{1}H NMR spectra of the crude bis(hexamolybdate) species are very similar to the spectrum of [n-$Bu_4N]_2[Mo_6O_{18}$(*p*-$MeOC_6H_4N$)] described above. The aromatic and O–CH_2– resonances are shifted downfield relative to those of the difunctional amines. The other methylene resonances of the ligands are difficult to assign because of their overlap with the tetrabutylammonium ion resonances. Integration of the ^{1}H NMR spectra provides three useful indicators of product composition: (i) since the crude products contain both unreacted aromatic amine functional groups (–C_6H_4–NH_2; upfield aromatic) and aryl imido ligands (–C_6H_4–N≡Mo_6O_{18}; downfield aromatic), the percentage of ArN units which are hexamolybdate bound can be determined; (ii) the ratio of arylimido ligands to hexamolybdate ions can be obtained by integrating the downfield aromatic resonances against the tetrabutylammonium ion resonances; (iii) the total ArN to hexamolybdate ion ratio can be determined by integrating both sets of aromatic resonances against the tetrabutylammonium ion resonances. This final ratio should be 1:1 if no materials are lost during work-up. Results from these integrations are reported in Table 5.

In each case, the (–C_6H_4–N≡Mo) to hexamolybdate ratio is significantly less than one-to-one indicating that significant quantities of unreacted [n-$Bu_4N]_2[Mo_6O_{19}$] are present in the crude products. Each product also gives a small set of aromatic and O–CH_2– resonances identical to those of the respective unreacted diamine. This suggests either that unreacted diamine is isolated with the product or that the organoimido ligands are hydrolytically unstable to work-up.

The IR spectra of the crude bis(hexamolybdate) species each show both the strong Mo–O stretch of the hexamolybdate ion at 950 cm^{-1} and a small shoulder at 974 cm^{-1} that is diagnostic for mono-organoimido substitution.

4. Conclusions

Aromatic amines with *para*-alkyloxy substituents react with the hexamolybdate ion to form arylimido adducts. *p*-Anisidine reacts with [n-$Bu_4N]_2[Mo_6O_{19}$] to give the [n-$Bu_4N]_2[Mo_6O_{18}$(*p*-$MeOC_6H_4N$)]$^{2-}$ adduct in reasonable (40%) yield and this product is readily purified through recrystallization. The products formed from reaction of [n-$Bu_4N]_2[Mo_6O_{19}$] with the related diamines, H_2N–C_6H_4–O–$(CH_2)_n$–O–C_6H_4–NH_2, also show clear evidence of arylimido ligand substitution. The conformational flexibility of these ligands holds great promise for the preparation of certain supramolecular species (e.g. the basket handle adducts mentioned above), for the preparation of soluble polymers,

Table 5
Compositions of the crude bis(hexamolybdate) species from ^{1}H NMR integration

Sample	% of ArN units that have been converted into arylimido ligands	Ratio of total ArN units to hexamolybdate ions	Ratio of (–C_6H_4–N≡Mo) units to hexamolybdate ions
Crude [n-$Bu_4N]_4[Mo_6O_{18}$N–C_6H_4–O–$(CH_2)_3$–O–C_6H_4–NMo_6O_{18}]	78	0.73:1	0.57:1
Crude [n-$Bu_4N]_4[Mo_6O_{18}$N–C_6H_4–O–$(CH_2)_4$–O–C_6H_4–NMo_6O_{18}]	79	0.89:1	0.71:1
Crude [n-$Bu_4N]_4[Mo_6O_{18}$N–C_6H_4–O–$(CH_2)_8$–O–C_6H_4–NMo_6O_{18}]	79	0.63:1	0.50:1

and for the attachment of polyoxometalates to solid supports. This same inherent flexibility may also contribute to our difficulty in crystallizing the products.

5. Supplementary material

Crystallographic data for the structural analysis have been deposited with the Cambridge Crystallographic Data Centre, CCDC No. 183903 for compound [n-Bu_4N]$_2$[Mo_6O_{18}(p-$MeOC_6H_4N$)]. Copies of the data may be obtained free of charge on application to The Director, CCDC, 12 Union Road, Cambridge, CB2 1EZ, UK (fax: +44-1223-336-033; e-mail: deposit@ccdc.cam.ac.uk or www: http://www.ccdc.cam.ac.uk).

6. Note added in proof

We recently discovered that A. Proust and R. Villanneau have also investigated the p-anisidine adduct, [Mo_6O_{18}(p-$MeOC_6H_4N$)]^2. Their discussion of its electronic structure can be found in: A. Proust and R. Villanneau, ''Functionalization of polyoxometalates: achievements and perspectives'', in: M.T. Pope and A. Müller (Eds.), Polyoxometalate Chemistry: From Topology via Self-Assembly to Applications, Kluwer, Dordrecht, 2001.

Acknowledgements

We would like to thank Dr. Todd Williams, Mr. Robert Drake, and Ms. Homigol Biesiada (University of Kansas, Molecular Structure Group) for their efforts in acquiring mass spectra. This research was supported by two Illinois Wesleyan University grants and the Illinois Wesleyan University Chemistry Department.

References

[1] (a) M.T. Pope, A. Müller (Eds.), Polyoxometalates: From Platonic Solids to Anti-Retroviral Activity, Kluwer, Dordrecht, 1994;
(b) C.L. Hill (Guest Ed.), Chem. Rev. 98 (1998) 1.;
(c) M.T. Pope, A. Müller (Eds.), Polyoxometalate Chemistry: From Topology via Self-Assembly to Applications, Kluwer, Dordrecht, 2001.

[2] (a) J.F. Hainfeld, C.J. Foley, L.E. Maelia, J.J. Lipka, J. Histochem. Cytochem. 38 (1990) 1787;
(b) J.F.W. Keana, M.D. Ogan, Y. Lü, J. Am. Chem. Soc. 107 (1985) 6714;
(c) J.F.W. Keana, M.D. Ogan, Y. Lü, M. Beer, J. Varkey, J. Am. Chem. Soc. 108 (1986) 7957.

[3] (a) S.-W. Zhang, Y.-G. Wei, Q. Yu, M.-C. Shao, Y.-Q. Tang, J. Am. Chem. Soc. 119 (1997) 6640;
(b) A.R. Moore, H. Kwen, A.M. Beatty, E.A. Maatta, Chem. Commun. (2000) 1793;
(c) C.R. Mayer, R. Thouvenot, T. Lalot, Chem. Mater. 12 (2000) 257.

[4] H. Zeng, G.R. Newkome, C.L. Hill, Angew. Chem., Int. Ed. Engl. 39 (2000) 1771.

[5] (a) J.B. Strong, G.P.A. Yap, R. Ostrander, L.M. Liable-Sands, A.L. Rheingold, R. Thouvenot, P. Gouzerh, E.A. Maatta, J. Am. Chem. Soc. 122 (2000) 639;
(b) W. Clegg, R.J. Errington, K.A. Fraser, S.A. Holmes, A. Schäfer, J. Chem. Soc., Chem. Commun. (1995) 455;
(c) Y. Wei, B. Xu, C.L. Barnes, Z. Peng, J. Am. Chem. Soc. 123 (2001) 4083;
(d) A. Proust, R. Thouvenot, M. Chaussade, F. Robert, P. Gouzerh, Inorg. Chim. Acta 224 (1994) 81;
(e) Y. Du, A.L. Rheingold, E.A. Maatta, J. Am. Chem. Soc. 114 (1992) 345.

[6] (a) J.B. Strong, R. Ostrander, A.L. Rheingold, E.A. Maatta, J. Am. Chem. Soc. 116 (1994) 3601;
(b) W.C. Clegg, R.J. Errington, K.A. Fraser, S.A. Holms, A. Schäfer, J. Chem. Soc., Chem. Commun. (1995) 455;
(c) J.L. Stark, A.L. Rheingold, E.A. Maatta, J. Chem. Soc., Chem. Commun. (1995) 1165.

[7] (a) A.R. Moore, Ph.D. Dissertation, Kansas State University, Mahattan, KS, 1998;
(b) A.R. Moore, H. Kwen, A.M. Beatty, E.A. Maatta, Chem. Commun. (2000) 1793;
(c) J.L. Stark, V.G. Young, Jr., E.A. Maatta, Angew. Chem., Int. Ed. Engl. 34 (1995) 2547.

[8] (a) B. Xu, Y. Wei, C.L. Barnes, Z. Peng, Angew. Chem., Int. Ed. Engl. 40 (2001) 2290;
(b) G. Hogarth, D.G. Humphrey, N. Kaltsoyannis, W.-S. Kim, M. Lee, T. Norman, S.P. Redmond, J. Chem. Soc., Dalton Trans. (1999) 2705.

[9] Y. Wei, B. Xu, C.L. Barnes, Z. Peng, J. Am. Chem. Soc. 123 (2001) 4083.

[10] N.H. Hur, W.G. Klemperer, R.-C. Wang, Inorg. Synth. 27 (1990) 77.

[11] M. Che, M. Fournier, J.P. Launay, J. Chem. Phys. 71 (1979) 1954.

[12] J. Bartulín, M.L. Ramos, B.L. Rivas, Polym. Bull. 15 (1986) 405.

[13] A.C. Griffin, T.R. Britt, R.S.L. Hung, M. Steele, Mol. Cryst. Liq. Cryst. 105 (1984) 305.

[14] B.V. Nonius, CAD4-Express Software, Ver. 5.1/1.2., Enraf–Nonius, Delft, The Netherlands, 1994.

[15] M. Kretschmar, GENHKL Program for the Reduction of CAD4 Diffractometer Data, University of Tübingen, Tübingen, Germany, 1997.

[16] A.C.T. North, D.C. Phillips, F.S. Mathews, Acta Crystallogr., A 24 (1968) 351.

[17] G.M. Sheldrick, Acta Crystallogr. A 46 (1990) 467.

[18] G.M. Sheldrick, SHELXL-97 Program for the Refinement of Crystal Structures, University of Göttingen, Göttingen, Germany, 1997.

[19] International Tables for Crystallography, vol. C, Kluwer Academic Publishers, Dordrecht, The Netherlands, 1995.

[20] A.L. Spek, PLATON, A Multipurpose Crystallographic Tool, Utrecht University, Utrecht, The Netherlands, 1998.

[21] J. Emsley, The Elements, 2nd ed., Clarendon Press, Oxford, 1991, p. 119.

[22] F. Bottomley, J. Chen, Organometallics 11 (1992) 3404.

[23] H. Kwen, V.G. Young, Jr., E.A. Maatta, Angew. Chem., Int. Ed. Engl. 38 (1999) 1145.

[24] T.-C. Hsieh, J.A. Zubieta, Polyhedron 5 (1986) 1655.

[25] S. Bank, S. Liu, S.N. Shaikh, X. Sun, J. Zubieta, P.D. Ellis, Inorg. Chem. 27 (1988) 3535.

[26] A. Proust, R. Thouvenot, F. Robert, P. Gouzerh, Inorg. Chem. 32 (1993) 5299.

[27] J.L. Stark, V.G. Young, Jr., E.A. Maatta, Angew. Chem., Int. Ed. Engl. 34 (1995) 5299.
[28] H. Kang, J. Zubieta, J. Chem. Soc., Chem. Commun. (1988) 1192.
[29] A. Proust, R. Thouvenot, P. Herson, J. Chem. Soc., Dalton Trans. (1999) 51.
[30] T.M. Che, V.W. Day, L.C. Francesconi, M.F. Fredrich, W.G. Klemperer, Inorg. Chem. 24 (1985) 4055.
[31] J. Fuchs, W. Freiwald, H. Hartl, Acta Crystallogr. B 34 (1978) 1764.
[32] Simple molecular mechanics calculations (using MM2 parameters in Personal CAChe) suggest that formation of basket handle species from the hexamolybdate ion and [n-Bu_4N]$_4$[$Mo_6O_{18}N$–C_6H_4–O–$(CH_2)_n$–O–C_6H_4–NMo_6O_{18}] diamines will be geometrically allowed if $n \geq 8$. The atomic positions of the Mo–O framework were taken from Maatta's X-ray data for [Mo_6O_{17}(N-Ar)$_2$]$^{2-}$ [5a] and those positions were locked for subsequent minimizations. The Mo≡N–C bond angles were fixed at 170° while the remainder of the organic ligand was geometrically unconstrained. The structures converged normally for $n \geq 8$. The eight-membered methylene strap had C–C single bond lengths of 1.54 Å and C–C–C bond angles ranging from 111.68 to 114.64°. While these angles are slightly greater than the tetrahedral angle, comparable bond angles have been observed in the polymethylene straps of other constrained, macrocyclic systems [33].
[33] M.W. Glogowski, Ph.D. Dissertation, The Ohio State University, Columbus, OH, 1988.